gation is not ideal. The origin of the diffuse scattering is not clear but an additional order of vacancies seems probable. The scattering has some of the features typical for vacancy ordering in transition-metal carbides (Sauvage & Parthé, 1972).

References

ANDERSSON, B. & GJØNNES, J. (1970). *Acta Chem. Scand.* **24**, 2250–2252.

ANDERSSON, B., GJØNNES, J. & TAFTØ, J. (1974). *Acta Cryst.* A**30**, 216–224.

CAMBINI, M., PELLEGRINI, G. & AMELINCKX, S. (1971). *Mater. Res. Bull.* **6**, 791–804.

DRITS, V. A., ORGANOVA, N. I. & DMITRIK, A. L. (1972). *Proc. Fifth European Congress on Electron Microscopy*, pp. 676–677.

GUINIER, A. (1963). *X-ray Diffraction.* San Francisco: Freeman.

HARADA, J. & KITAMURA, M. J. (1964). *J. Phys. Soc. Japan*, **19**, 328–343.

ROSTOKER, W. & YAMAMOTO, A. S. (1955). *Trans. Amer. Soc. Metals*, **47**, 1002–1017.

SAUVAGE, M. & PARTHÉ, E. (1972). *Acta Cryst.* A**28**, 607–616.

STRINGER, J. (1965). *J. Less-Common Metals*, **8**, 1–14.

UDALOVA, V. V. & PINSKER, Z. G. (1964). *Sov. Phys. Crystallogr.* **8**, 433–440.

VAINSHTEIN, B. K. (1964). *Structure Analysis by Electron Diffraction.* Translated by E. FEIGL & J. A. SPINK. Oxford: Pergamon Press.
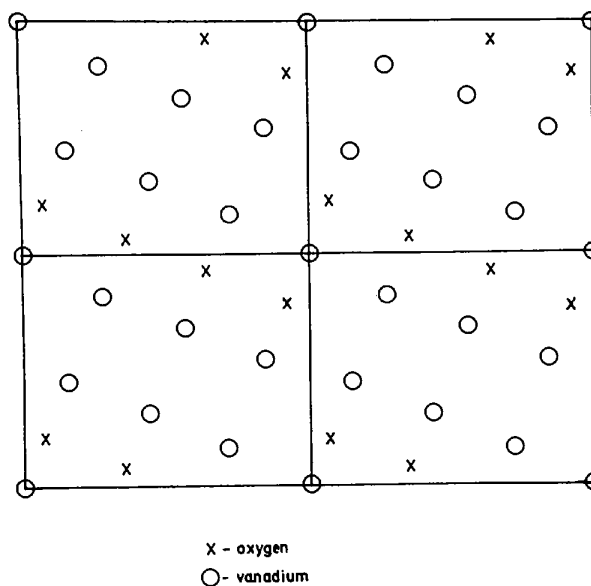
X - oxygen

O - vanadium

Fig. 8. The (010) plane of the proposed structure which corresponds to {110} or {100} of the NaCl and b.c.c. types of structure respectively. Full, heavy lines outline the unit cell of the γ phase.

WESTMAN, S. (1963). *Acta Chem. Scand.* **19**, 749–752.

WESTMAN, S. & NORDMARK, C. (1960). *Acta Chem. Scand.* **14**, 465–470.

Identification of Enantiomorphism in Crystals by Electron Microscopy

BY OMER VAN DER BIEST AND G. THOMAS

Inorganic Materials Research Division, Lawrence Berkeley Laboratory and Department of Materials Science and Engineering, College of Engineering, University of California, Berkeley, California, U.S.A.

Simple electron-microscopy techniques are described which allow one to detect the presence of two enantiomorphous forms of a structure within an apparent single crystal. The first method consists of a characterization of the interface between the two enantiomorphs. In the second method advantage is taken of violations of Friedel's law which can occur in non-centrosymmetric crystals. These techniques have been illustrated by an analysis of the domain structure in ordered $LiFe_5O_8$, which has a space group $P4_132$ or $P4_332$. Consistent results were obtained with both methods. The first method yields a more complete description of the domain structure. Methods which can be used to determine the absolute configuration of the structure in a part of the crystal are discussed.

1. Introduction

When a structure belongs to a space group which does not contain a symmetry operation of the second sort, that is an operation which does not involve an inversion or a reflection, then it can exist in either a right-handed or a left-handed form. In some cases these two forms have different space groups, which are an enantiomorphous pair of space groups. With ordinary X-ray diffraction techniques it is impossible to distinguish between these two enantiomorphous forms. It is necessary to include anomalous scattering in the calculations and often very accurate intensity measurements are necessary. The use of anomalous scattering of X-rays to determine the absolute configuration of a structure has been reviewed by Rama-

seshan (1964). Recent contributions to this field include the use of the shape of X-ray intensity spectra (Burr & Woods, 1973) and applications of the Kossel effect (Brümmer, Beier & Neiber, 1973).

These X-ray methods have their limitations. The structure should contain at least two different species, one of which should be an anomalous scatterer. The latter condition cannot always be fulfilled with commonly available X-ray wavelengths, for instance, if a structure contains only light elements. Iwasaki (1974) has shown that there may be some, so far imaginary, non-centrosymmetric structures, for which Friedel's law holds even with anomalous dispersion. In addition, one would have to be sure that both forms of the structure do not coexist on a very fine scale, *viz.* smaller than the diameter of an X-ray beam, within an apparent single crystal. This will depend on whether or not it is possible to have a low-energy interface between the two structures, when the crystal axes in both remain parallel.

In this paper it will be shown that if both enantiomorphous forms do occur in the form of very small domains, the presence of the right and left-handed forms can be confirmed by contrast experiments in the electron microscope. Two different methods have been used, the first method consists of an analysis of the interface between the two structures. This interface can be described by a set of geometrical operations which convert the structure on one side into the structure on the other side of the interface. With simple contrast experiments it can be ascertained whether or not the operations characterizing the interface contain an inversion operation. A similar method of analysis was used by McLaren & Phakey (1966) in a study of Brazil twinning in quartz. The second method which can be used to confirm the results of the first, takes advantage of a violation of Friedel's law in electron diffraction. Exceptions to Friedel's law in electron diffraction were first observed by Thiessen & Molière (1939) and later by Miyake & Uyeda (1950). A theoretical discussion of Friedel's law in n-beam dynamical theory was given by Fujimoto (1959), Cowley & Moodie (1959) and recently by Serneels, Snykers, Delavignette, Gevers & Amelinckx (1973), who specifically considered the contrast between domains related by an inversion operation in non-centrosymmetric crystals.

2. Structural information

The compound which has been studied is ordered $LiFe_5O_8$. The structure goes through a phase transformation above 750°C, which has been shown to be of the order–disorder type (Braun, 1952). The disordered structure has the inverse spinel structure (space group $Fd3m$, lattice parameter $a = 8.33$ Å), with Fe^{3+} on the tetrahedrally coordinated sites and a mixture of Li^+ and $3Fe^{3+}$ on the octahedrally coordinated sites. Below 750°C, Li^+ and Fe^{3+} order and the space-group

symmetry is lowered to $P4_132$ or $P4_332$. This is accompanied by a slight change in lattice parameter (Brunel & de Bergevin, 1964). The atomic coordinates for the ions used in this work were given by Braun (1952) using the equivalent positions for $P4_332$ (No. 212, *International Tables for X-ray Crystallography*, 1969): 4 Li at (b); 12 Fe at (d) with $x = \frac{3}{8}$; 8 Fe at (c) with $x = 0$; 24 oxygen at (c) with $x = \frac{1}{8}$, $y = -\frac{1}{8}$, $z = \frac{1}{8}$, 8 oxygen at (c) with $x = \frac{3}{8}$. Small corrections for these coordinates were neglected, *i.e.*, we assumed that the disordered structure is an ideal spinel structure. The complete set of coordinates of the octahedral sites is given in Table 1. A projection of these sites on the (100) plane is given in Fig. 1.

Table 1. *Coordinates of octahedral sites*

No.	x	y	z
1	0·625	0·625	0·625
2	0·125	0·875	0·375
3	0·375	0·125	0·875
4	0·875	0·375	0·125
5	0·125	0·375	0·875
6	0·875	0·125	0·375
7	0·375	0·875	0·125
8	0·375	0·625	0·375
9	0·375	0·375	0·625
10	0·625	0·375	0·375
11	0·625	0·125	0·125
12	0·125	0·625	0·125
13	0·125	0·125	0·625
14	0·875	0·875	0·625
15	0·625	0·875	0·875
16	0·875	0·625	0·875

Considering now one space group only, it can be seen from Fig. 1 that the set of octahedral sites can be divided into four subsets, one of which contains only lithium ions and the other three only iron ions. When ordering sets in, the lithium ions can occupy any of these four subsets. After ordering, the single crystal is fragmented into domains in a way similar to ordered metallic phases (*e.g.*, see Marcinkowski, 1961). Within each domain, the lithium ions will occupy only one subset and at the boundary between domains they will be out of phase. These boundaries can be described by the vector which translates the lithium ions from one subset to another. A $\frac{1}{2}\langle 110 \rangle$ type vector is a lattice vector of the disordered structure, hence, a translation of the ordered structure over this vector does not affect the oxygen ions or iron ions in tetrahedral sites, but it does transfer the Li ions from one subset to another. This holds for either one of the space groups.

There are thus actually eight different subsets out of the 16 octahedral sites which the Li ions can occupy, and it is possible to have a boundary between any pair of these. The eight arrangements are enumerated in Table 2. The arrangements $1L$ and $1R$ have been taken rather arbitrarily as 'basic' arrangements for $P4_332$ and $P4_132$ respectively. These two arrangements

can be brought into coincidence with one another by an inversion through the point $(\frac{5}{8},\frac{5}{8},\frac{5}{8})$, hence the boundary between these two arrangements will be called an inversion boundary. On the other hand, a boundary between $1L$ and $2R$ would not only involve an inversion through $(\frac{5}{8},\frac{5}{8},\frac{5}{8})$ but also a translation over a vector $\frac{1}{2}[110]$.

Table 2. *Atomic coordinates of the eight ordered arrangements*

Symbol	Arrangement	Atomic coordinates*
$1L$	$P4_332$	Li: 1, 2, 3, 4†
$2L$	$P4_332+\frac{1}{2}[110]‡$	Li: 7, 10, 13, 16
$3L$	$P4_332+\frac{1}{2}[101]$	Li: 6, 9, 12, 15
$4L$	$P4_332+\frac{1}{2}[011]$	Li: 5, 8, 11, 14
$1R$	$P4_132$	Li: 1, 5, 6, 7
$2R$	$P4_132+\frac{1}{2}[110]$	Li: 4, 8, 13, 15
$3R$	$P4_132+\frac{1}{2}[101]$	Li: 3, 10, 12, 14
$4R$	$P4_132+\frac{1}{2}[011]$	Li: 2, 9, 11, 16

* The octahedral sites not occupied by lithium are occupied by the iron ions. Only the positions of the lithium ions are given. The positions of the oxygen ions and tetrahedral ions are the same for all the ordered arrangements.

† These numbers refer to the numbers of the octahedral sites as given in Table 1.

‡ $P4_332+\frac{1}{2}[110]$ means that this arrangement is derived from the 'basic' $P4_332$ arrangement by giving the Li ions a displacement over a vector $\frac{1}{2}[110]$.

This description of the boundaries is not unique. In principle, each boundary involving an inversion can be described as a pure inversion boundary by proper choice of the inversion point. Here the inversion point is considered to be fixed. In the context of this paper 'inversion' means inversion through the point $(\frac{5}{8},\frac{5}{8},\frac{5}{8})$. The boundaries could also be described by means of a reflection operation, for instance with respect to the (110) planes, which may or may not be accompanied by a translation.

One could have a total of 28 boundaries between the eight possible arrangements. However, only seven boundaries, distinct in the geometrical operations characterizing them, can occur. These boundaries are indicated schematically in Fig. 2. There are three translation boundaries, one inversion boundary and three boundaries described by an inversion and a translation. All 28 boundaries are enumerated and classified in Table 3.

Table 3. *Classification of boundaries*

Symbols used in this table are explained in Table 2 and in Fig. 2.

T_1	T_2	T_3	I	$I+T_1$	$I+T_2$	$I+T_3$
$1L–2L$	$1L–3L$	$1L–4L$	$1L–1R$	$1L–2R$	$1L–3R$	$1L–4R$
$3L–4L$	$2L–4L$	$2L–3L$	$2L–2R$	$2L–1R$	$2L–4R$	$2L–3R$
$1R–2R$	$1R–3R$	$1R–4R$	$3L–3R$	$3L–4R$	$3L–1R$	$3L–2R$
$3R–4R$	$2R–4R$	$2R–3R$	$4L–4R$	$4L–4R$	$4L–2R$	$4L–1R$

$P4_332$

$P4_132$

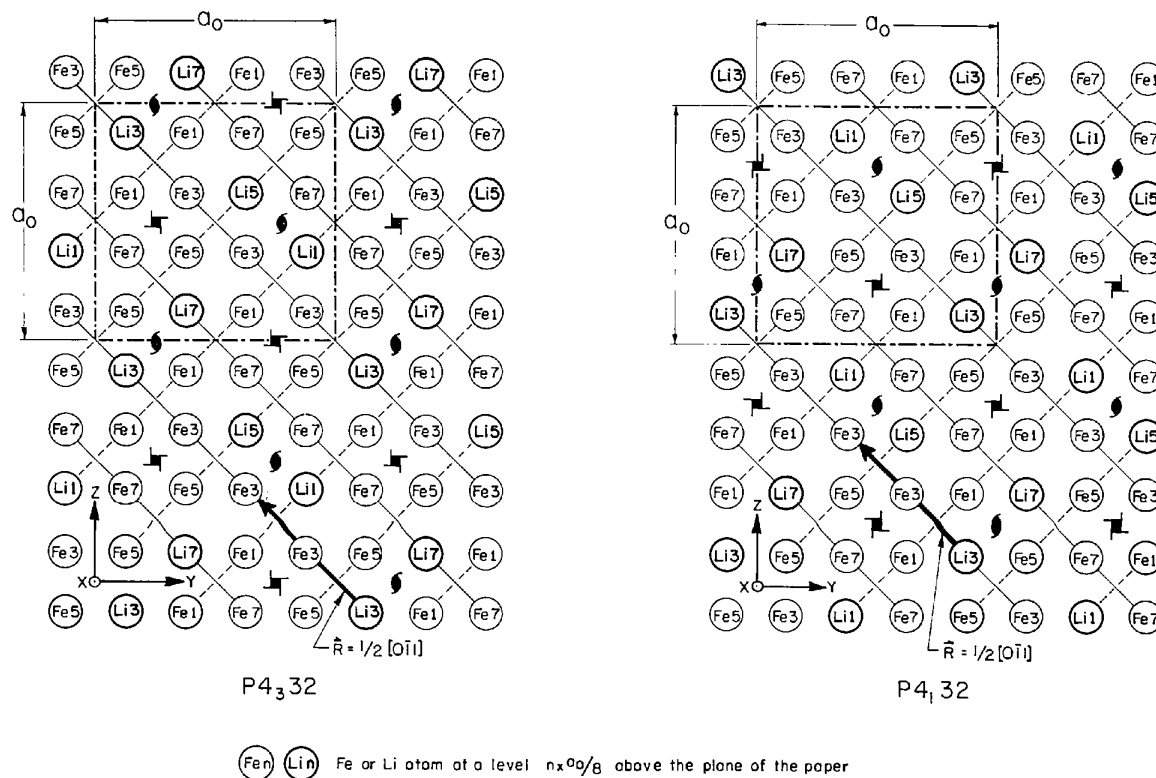Fe or Li atom at a level $n_x a_0/8$ above the plane of the paper

Fig. 1. Projection of the octahedral sites on the (100) plane for the two enantiomorphs. The unit cell indicated is the conventional one for the $P4_332$ spacegroup. It is indicated how the octahedral sites are aligned in $\langle 011\rangle$ directions with one Li ion followed by three Fe ions.

The ordered and disordered structures contain stacking faults. It was shown by Van der Biest & Thomas (1974) that these faults lie on $\{110\}$ planes and have a displacement vector of $\frac{1}{4}\langle 110 \rangle$, which is always perpendicular to the fault plane. It will be shown that in the ordered structure an inversion can occur at these faults.

3. Contrast in the electron microscope

3.1. Contrast at domain boundaries

It is useful to reconsider here the two-beam dynamical theory of contrast at a stacking fault in crystals [e.g., see Whelan & Hirsh (1957); Hirsch, Howie, Nicholson, Pashley & Whelan (1965). The equations for the faulted crystal can be derived from those of the perfect crystal simply by modifying the Fourier coefficient of the crystal potential in the bottom part of the crystal by a phase factor $\exp(i\alpha)$, i.e.,

$$V_g^b = V_g^t \exp (i\alpha) \qquad (1)$$

where b indicates the bottom of the crystal and t indicates the top (facing the electron beam). $\alpha = -2\pi g.R$, where R is the displacement of the bottom relative to the top and g is the reciprocal-lattice vector corresponding to the reflection excited. It is understood here that the potential of the top of the crystal $V^t(r)$ and the potential at the bottom $V^b(r)$ have both been referred to the same origin. Equation (1) implies that:

$$F_g^b = F_g^t \exp (i\alpha) . \qquad (2)$$

This equation yields another interpretation for the phase angle α: α is the difference between the phase angles in the structure factor expressions for the top and bottom of the crystal, calculated with respect to a common origin.

In the case of a boundary between a left-handed and a right-handed crystal, we can write quite generally the following expression for the structure factor:

$$F_g^l = |F_g^l| \exp (i\alpha_g^l) \qquad F_g^r = |F_g^r| \exp (i\alpha_g^r) .$$

In particular, for the moduli of the structure factor it follows regardless of choice origin:
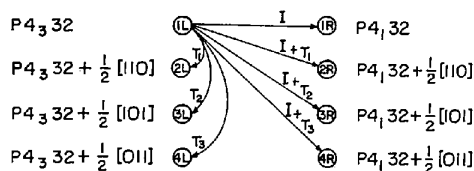
$$|F_g^l| = |F_g^r| .$$

P4₃32

$P4_3 32 + \frac{1}{2}[110]$

$P4_3 32 + \frac{1}{2}[10\bar{1}]$

$P4_3 32 + \frac{1}{2}[01\bar{1}]$

P4₁32

$P4_1 32 + \frac{1}{2}[110]$

$P4_1 32 + \frac{1}{2}[10\bar{1}]$

$P4_1 32 + \frac{1}{2}[01\bar{1}]$

Fig. 2. Schematic representation of the seven different boundaries in ordered LiFe₅O₈. The labels of the ordered arrangements are explained in Table 2.

Hence, it follows that:

$$F_g^l = F_g^r \exp [i(\alpha_g^l - \alpha_g^r)]$$

or

$$F_g^l = F_g^r \exp (i\alpha) \qquad (3)$$

with

$$\alpha = \alpha_g^l - \alpha_g^r . \qquad (4)$$

If now a boundary between the two enantiomorphs is considered with the right-handed structure at the top of the crystal facing the electron gun and the left-handed structure at the bottom, equation (3) implies that

$$V_g^l = V_g^r \exp (i\alpha) . \qquad (5)$$

Hence, the relationship between the crystal potential in the two parts of the crystal on either side of this boundary is the same as in the case of a stacking fault. The results of the two-beam dynamical theory of contrast at a stacking fault apply equally well to this boundary. A boundary between two enantiomorphs will be imaged as α fringes where α is now equal to the difference in the phase angle of the structure-factor expression calculated with respect to the same origin. This phase difference is independent of the actual choice of origin.

In the dynamical theory of contrast the assumption is usually made that the crystal is centrosymmetric so that one can write $V_g = V_{-g}$ (or $F_g = F_{-g}$). In a two-beam case this assumption is not really necessary as one is free to chose the origin so that for a particular beam $F_g^t = F_{-g}^t = F_g^t*$ which means that in the example above $\alpha_g^r = 0$. It is clear that this approach to the contrast problem at an inversion boundary will not be valid in the case of a many-beam situation, because it is then not possible to choose an origin so that the condition $V_g = V_{-g}$ is simultaneously fulfilled for all the beams involved.

Using a simple structure-factor program, the values of α were calculated for each of the seven boundaries which occur in ordered LiFe₅O₈. The atomic coordinates for the iron and lithium ions on the octahedral sites given in Table 2 were used. The results are shown in Table 4. In the case of translation boundaries the value of α is also equal to $-2\pi g . R$. Wherever $\alpha = 0$ or 2π, a domain boundary will be out of contrast. For reflections of the type 110, 211, 103, 123, α takes the value 0, π. For reflections of the type 102, 302 α takes the value 0, π for translation boundaries but only $\pm \pi/2$ for inversion boundaries. For all spinel reflections $\alpha = 0$ and the boundaries should be out of contrast.

3.2. Contrast between domains

In a second method, by which the presence of two enantiomorphous structures can be verified, one takes advantage of the violations in Friedel's law which take place in electron diffraction in certain multiple-beam situations. What is meant by a violation of Friedel's law is that $+g$ and $-g$ do not have the

Table 4. *Values of the phase angle* α

C	T_1	T_2	T_3	I	$I+T_1$	$I+T_2$	$I+T_3$
110	0	π	π	0	0	π	π
1̄10	0	π	π	π	π	0	0
101	π	0	π	0	π	0	π
10̄1	π	0	π	π	0	π	0
011	π	π	0	0	π	π	0
01̄1	π	π	0	π	0	0	π
112	0	π	π	0	0	π	π
1̄12	0	π	π	π	π	0	0
11̄2	0	π	π	π	π	0	0
1̄1̄2	0	π	π	0	0	π	π
211	π	π	0	0	π	π	0
21̄1	π	π	0	π	0	0	π
2̄11	π	π	0	π	0	0	π
2̄1̄1	π	π	0	0	π	π	0
121	π	0	π	0	π	0	π
12̄1	π	0	π	π	0	π	0
1̄21	π	0	π	π	0	π	0
1̄2̄1	π	0	π	0	π	0	π
1̄20	π	π	0	$\pi/2$	$-\pi/2$	$-\pi/2$	$\pi/2$
120	π	π	0	$-\pi/2$	$\pi/2$	$\pi/2$	$-\pi/2$
210	π	0	π	$\pi/2$	$-\pi/2$	$\pi/2$	$-\pi/2$
2̄10	π	0	π	$\pi/2$	$-\pi/2$	$\pi/2$	$-\pi/2$
021	0	π	π	$\pi/2$	$\pi/2$	$-\pi/2$	$-\pi/2$
02̄1	0	π	π	$\pi/2$	$\pi/2$	$-\pi/2$	$-\pi/2$
012	π	0	π	$-\pi/2$	$\pi/2$	$-\pi/2$	$\pi/2$
01̄2	π	0	π	$\pi/2$	$-\pi/2$	$\pi/2$	$-\pi/2$
102	π	π	0	$\pi/2$	$-\pi/2$	$-\pi/2$	$\pi/2$
1̄02	π	π	0	$-\pi/2$	$\pi/2$	$\pi/2$	$-\pi/2$
201	0	π	π	$-\pi/2$	$-\pi/2$	$\pi/2$	$\pi/2$
20̄1	0	π	π	$\pi/2$	$\pi/2$	$-\pi/2$	$-\pi/2$

5. Results

From systematic extinctions in the precession photographs it was confirmed that the space group of the disordered structure is $Fd3m$. The precession photographs of the ordered compound showed the presence of systematic extinctions required for the space groups $P4_132$ and $P4_332$. The non-systematic extinctions in these photographs could be accounted for by the atomic positions given by Braun (1952).

Fig. 3 shows a series of transmission electron micrographs taken under a variety of diffraction conditions. Fig. 3(a) was taken under conditions approaching a two-beam case as the $0\bar{2}4$ and $02\bar{4}$ reflections are not allowed. Fig. 3(b), (c) and (d) were taken with a systematic row of reflections operating with the indicated reflection on the Ewald sphere. Although the presence of the systematic beams will alter the detail of the contrast at the boundary, it will not affect the visibility criteria derived for two-beam conditions. The visibility or invisibility of the boundaries marked by a lower-case letter in Fig. 3(a) has been tabulated in Table 5. Comparison of these results with the calculations given in Table 4 allows one to identify each of the boundaries with one of the seven types of boundaries possible. This identification is made in the last column of Table 5.

same intensity even when the excitation errors are the same. At an inversion boundary, when $+g$ is operating in one part of the crystal $-g$ is operating in the inverted part with exactly the same excitation. When Friedel's law is violated then the domains should show up with different intensities. This situation was studied by Serneels *et al.* (1973) and they concluded the following: (i) A multi-beam condition is necessary to observe any contrast at all. (ii) Friedel's law holds for the direct beam in a general multiple-beam situation. It does not hold in general in dark field. (iii) The difference in intensity depends strongly on the thickness of the crystal. (iv) If the only reflections excited belong to a zone axis along which the crystal displays a center of symmetry in projection, no contrast should be observed in dark field.

4. Experimental techniques

The specimens studied were flux-grown single crystals of $LiFe_5O_8$. A Buerger precession camera was used to check the space-group symmetry of the structures involved. The specimens used for this study were annealed at 850 °C and furnace cooled. Standard thin sections were prepared. Final thinning was done using an ion-bombardment technique (Barber, 1970) or by chemically polishing in hot phosphoric acid. The specimens were examined in a Hitachi HU-650 microscope operated at 650 kV.

Table 5. *Analysis of Fig. 3*

Boundary*	g=1̄10	g=01̄1	g=1̄01	Type
a	NC†	NC	C‡	$I+T_2$
b	NC	C	C	T_1
c	NC	C	NC	$I+T_3$
d	C	NC	C	T_3
e	NC	C	NC	$I+T_3$
f	C	NC	NC	$I+T_1$
g	NC	C	C	T_1
h	C	NC	NC	$I+T_1$
i	C	C	NC	T_2
j	C	C	NC	T_2
k	C	NC	NC	$I+T_1$
l	NC	C	NC	$I+T_3$

* The boundaries are labeled in Fig. 3(a).
† *NC*: boundary not in contrast.
‡ *C*: boundary in contrast.

The internal consistency of the method of analysis can be checked by labeling each domain as follows: because at present, these electron-microscopic methods do not yet allow the determination of the absolute configuration, it was assumed that the domain which runs vertically through the micrograph has a left-handed $P4_332$ arrangement. It was also assumed that it was the 'basic' $1L$ arrangement. The latter assumption is equivalent to choosing an origin. Once these assumptions are made, the arrangements in all the other domains can be found through the character of their boundaries derived in Table 5, and the use of
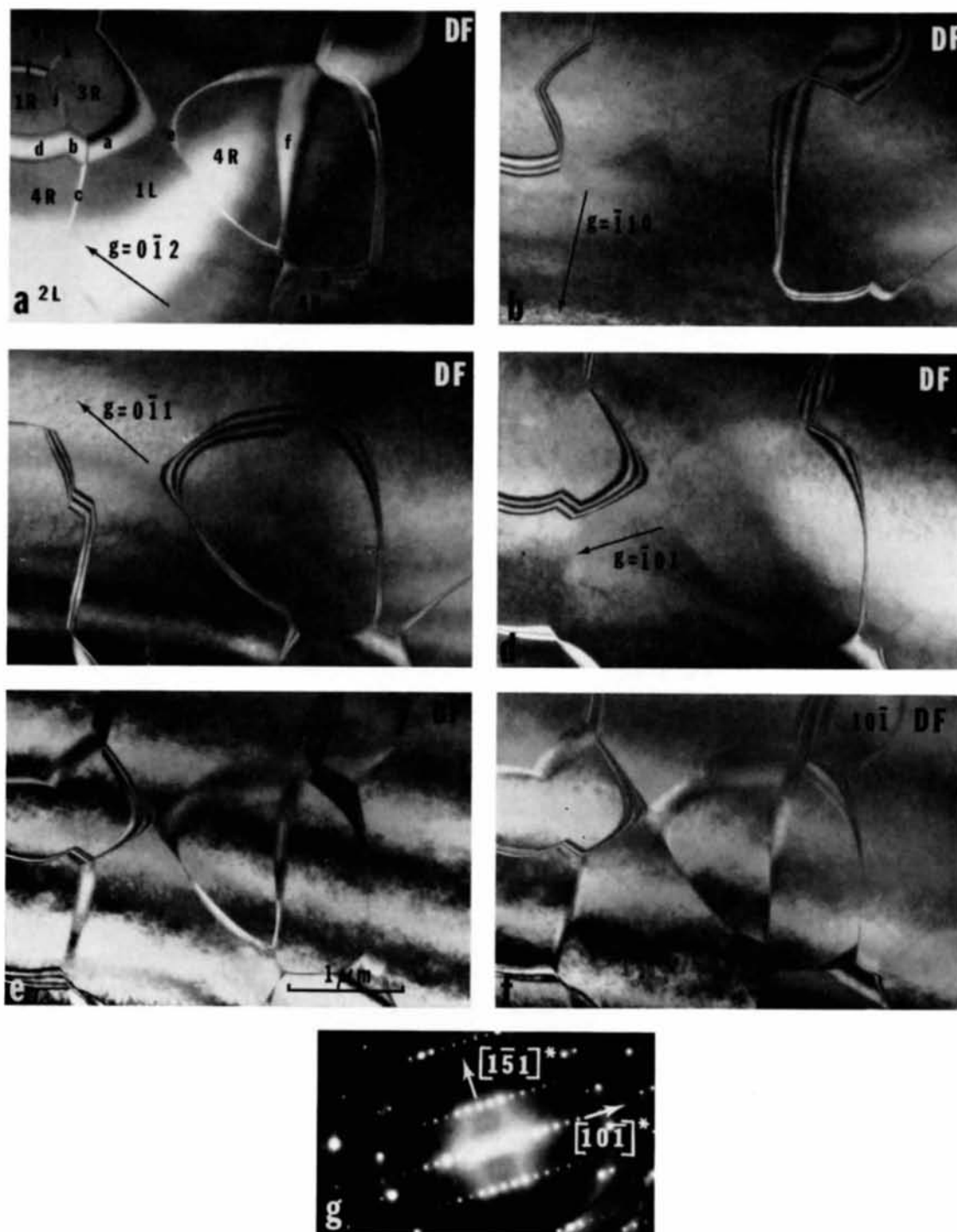
Fig. 3. An identical area of an ordered crystal photographed under five different diffraction conditions. The operating reflections in (*a*), (*b*), (*c*) and (*d*) are indicated by vectors. The diffraction pattern corresponding to (*e*) and (*f*) is shown in Fig. (*g*) (BF: bright field; DF: dark field with reflection used indicated).
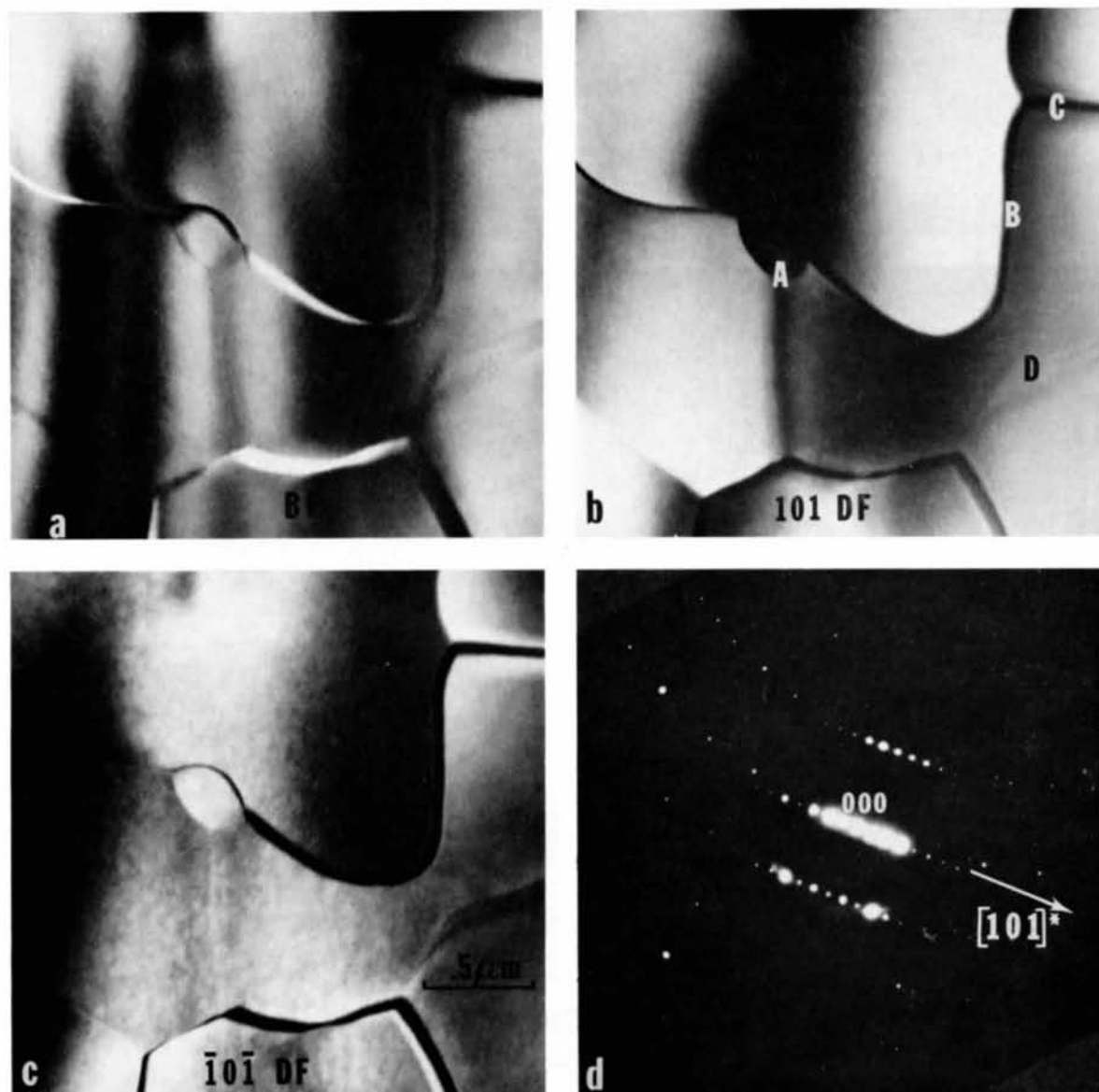
Fig. 4. Bright field (*a*) and two dark fields (*b*, *c*) showing that a few fairly strong reflections off the operating row are sufficient to produce strong differences in contrast between enantiomorphic domains (*e.g.* at *A* and *B*). Across translation boundaries there is no difference in background intensity (*e.g.* at *C* and *D*).
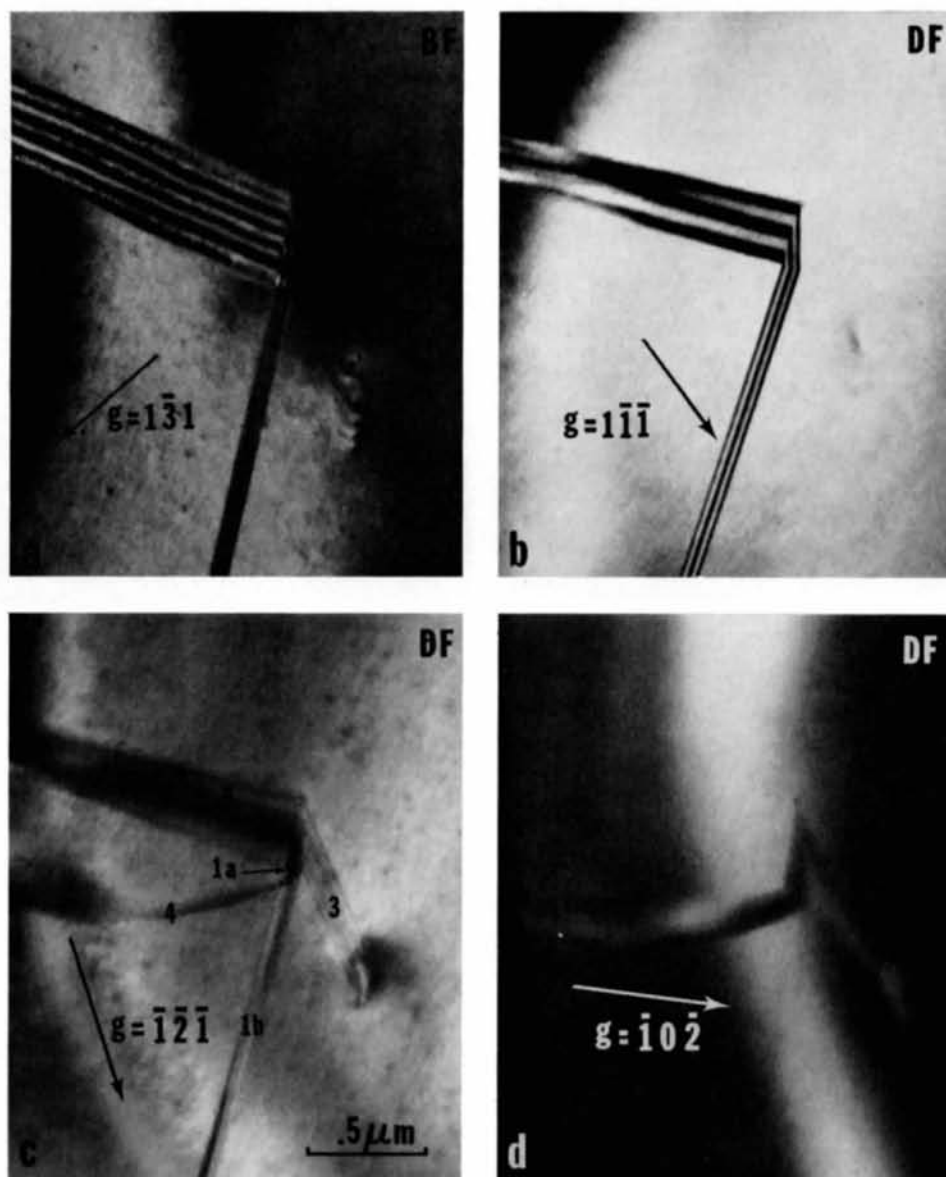
Fig. 5. Three stacking faults forming a triple junction in ordered lithium ferrite. The same area was photographed under four different diffraction conditions, characterized by the g vectors in the figures.
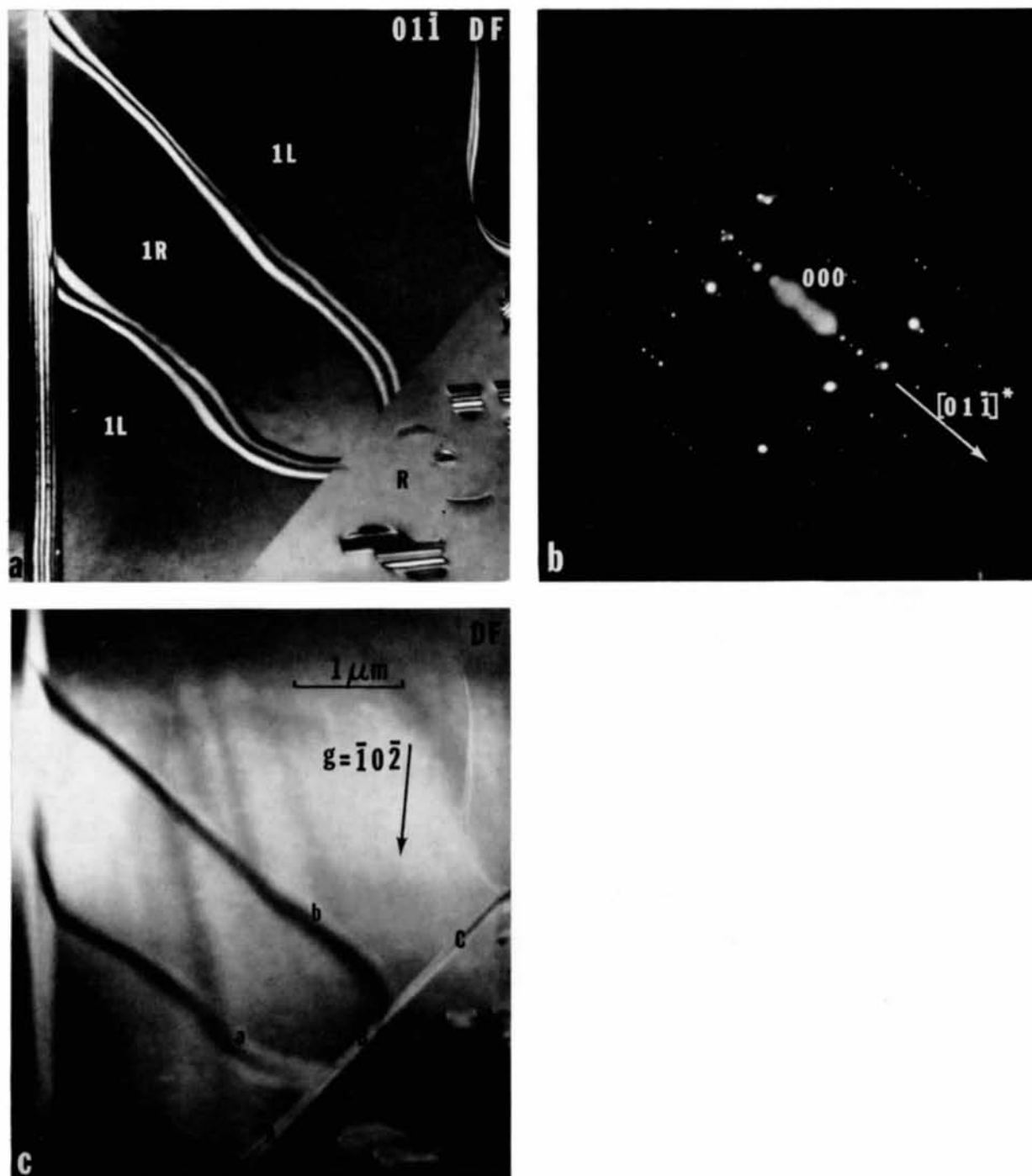
Fig. 6. (a) was taken under the conditions shown in (b). (c) was taken under the diffraction conditions indicated in the figure.

Table 3. This was done in Fig. 3(a). This labeling of domains provides a check on the identification of the boundaries, e.g., if a is a boundary between 1L and 3R and b is a boundary between 3R and 4R, then clearly the character of c is fixed and c has to behave as a 1L−4R boundary, i.e., I+T₃. This has indeed been found by contrast experiments (Table 5). Hence, a complete internally consistent picture is obtained of the relationships between the domains.

An independent check on these results is provided in Fig. 3(e), (f) and (g). The same area was imaged here under multi-beam conditions [Fig. 3(g)], hence one may expect violations of Friedel's law at inversion boundaries. The foil was wedge-shaped with thinner parts at the bottom of the pictures. The fringes in Fig. 3(e) running from right to left are thickness fringes. These remain continuous across the boundaries in the bright-field picture. In dark field, however, these fringes change color at some boundaries (e.g. at a and c) but remain continuous across others (e.g. at j and g). The latter ones may be expected to be translation boundaries whereas the first should be inversion boundaries. Comparison with Fig. 3(a) shows that these boundaries are the same ones for which the first method showed that an inversion was involved.

Fig. 4 provides another example where the two enantiomorphous structures can be distinguished by a difference in background intensity. This specimen was chemically thinned and some etching had occurred at the boundaries. The presence of two strong 'accidental' reflections was sufficient to provide a very strong contrast between enantiomorphous domains, e.g. at A and B. There is no difference in background intensity across translation boundaries, e.g. at C and D.

Fig. 5 shows three stacking faults on {110} planes meeting along a line. The displacement vector of these faults was determined as $\frac{1}{4}\langle 110 \rangle$ plus a spinel lattice vector. The boundary 4 joining fault 1 is a translation boundary. The contrast in Fig. 5(d) can be explained only if faults 1 and 2 are simultaneously boundaries between the left and right-handed structures. The displacement vectors of these faults are: $R_{1a}=\frac{1}{4}[10\bar{1}]$, $R_{1b}=\frac{1}{4}[\bar{1}0\bar{1}]$, $R_2=\frac{1}{4}[110]$. For $g=\bar{1}0\bar{2}$, this yields for the phase angle $\alpha_{1a}=\pi/2$, $\alpha_{1b}=-\pi/2$ and $\alpha_2=-\pi/2$. Hence, if these faults were simple translation faults, they should be visible as α fringes with $\alpha=\pm\pi/2$. If these faults also included an inversion operation then a phase angle of $\pm\pi/2$ would be added (see Table 4). Taking the plus sign yields: $\alpha_{1a}=\pi$, $\alpha_{1b}=0$ and $\alpha_2=0$. Hence, the b parts of fault 1 and fault 2 will be invisible. This matches the observations.

Additional evidence that stacking faults can also serve as the boundary between enantiomorphous forms is given in Fig. 6. Fig. 6(a) was taken under the diffraction conditions shown in Fig. 6(b). Fig. 6(c) shows that the fault ABC seen edge on in (a) is indeed a stacking fault. Analysis of the boundaries a and b showed that they were pure inversion boundaries. The difference in background contrast at A and C indicates

that an inversion takes place at the stacking fault. However, there should not be any difference in background intensity at B. This is indeed observed.

6. Discussion

The domain size in the ordered crystal depends on the heat treatment but is usually of the order of 1μm or smaller, and, hence well below the diameter of an X-ray beam. It is clear that a very fine intergrowth of the two enantiomorphous structures would give rise to a spurious center of symmetry in diffraction even when an X-ray wavelength is used for which iron is a strong anomalous scatterer. The success of the electron-microscopic methods does not depend on the presence of a particular atomic species in the compound. The method should also be applicable for structures containing only light-weight elements.

In the multibeam method, the contrast in dark field arises from a complex interaction between n beams. However, one cannot show in general that the difference in intensity between the inverted domains will be large enough to be detectable. This difference in intensity will depend on the details of the structure, the thickness of the sample and the diffraction conditions. It is shown by Serneels et al. (1973) that for very thick foils the contrast will be destroyed by absorption.

The analysis of an inversion boundary using different g vectors should be applicable to all crystals in which enantiomorphous domains occur. The success of this method hinges on the fact that there is a difference in phase angle of a particular reflection for the two enantiomorphous structures when both are referred to the same reference frame. Reflections for which this phase-angle difference is not equal to zero can always be found. This method has the additional advantage that it yields a complete description of the interface between the two structures. Not only can it be established that an inversion operation is involved at the boundary but any additional translation can be determined as well. In general, these translations are not known a priori. In the case of ordered LiFe₅O₈ a precise description of the domain structure can be given because the ordered structure is derived from the relatively simple spinel structure. This is the reason why lithium ferrite forms an ideal case to illustrate the use of these electron microscopic techniques.

For all practical purposes it might be sufficient to establish the presence of the two enantiomorphous forms within an apparent single crystal. The microscopic methods described in this paper have not yet been extended to determine the absolute configuration of the structure in a part of the crystal. In principle this possibility exists. In the case of the multibeam method, one should be able to predict, using a many beam dynamical theory for non-centrosymmetric crystals, which form should show up bright in dark field for a given crystal thickness and diffraction condition. In general, an electronic computer would have to be

used for this. The problem is completely analogous to the absolute determination of the orientation of a non-centrosymmetric crystal, which has reflection symmetry. This problem has been solved for hexagonal CdS by Goodman & Lehmpfuhl (1968), who used a convergent-beam technique and a multiple-slice calculation for n-beam diffraction.

In the case of the interface analysis, it should be possible to predict for an interface inclined with respect to the beam which form is at the top of the crystal facing the electron gun. This can only be done when the difference in phase angle α is different from π. In the case of ordered lithium ferrite this is the case for reflections of type 012 or 203 when $\alpha = \pm \pi/2$. The problem is then reduced to a determination of the character of a stacking fault in f.c.c. metals (Hirsch, et al., 1965). A systematic study of this problem for $\alpha = \pi/2$ has not yet been undertaken.

References

BARBER, D. J. (1970). J. Mater. Sci. 5, 1–8.
BRAUN, P. B. (1952). Nature, Lond. 170, 1123.
BRÜMMER, O., BEIER, W. & NEIBER, H. (1973). Phys. Stat. Sol. (a), 20, K119–K121.

BRUNEL, M. & DE BERGEVIN, F. (1964). C. R. Acad. Sci. Paris, 258, 5628–5631.
BURR, K. F. & WOODS, J. (1971). J. Mater. Sci. 6, 1007–1011.
COWLEY, J. M. & MOODIE, A. F. (1959). Acta Cryst. 12, 360–367.
FUJIMOTO, F. (1959). J. Phys. Soc. Japan 14, 1558–1568.
GOODMAN, P. & LEHMPFUHL, C. (1968). Acta Cryst. A24, 339.
HIRSCH, P. B., HOWIE, A., NICHOLSON, R. B., PASHLEY, D. W. & WHELAN, M. J. (1965). Electron Microscopy of Thin Crystals. London: Butterworth.
International Tables for X-ray Crystallography (1969). Vol. I. Birmingham: Kynoch Press.
IWASAKI, H. (1974). Acta Cryst. A30, 173–176.
McLAREN, A. C. & PHAKEY, P. P. (1966). Phys. Stat. Sol. 13, 413–421.
MARCINKOWSKI, M. J. (1961) in Electron Microscopy and Strength of Crystals, Edited by G. THOMAS & J. WASHBURN, pp. 333–437. New York: Interscience.
MIYAKE, S. & UYEDA, R. (1950). Acta Cryst. 3, 314.
RAMASESHAN, S. (1964). in Advanced Methods in Crystallography, Edited by S. RAMACHANDRAN, pp. 67–95. New York: Academic Press.
SERNEELS, R., SNYKERS, M., DELAVIGNETTE, P., GEVERS, R. & AMELINCKX, S. (1973). Phys. Stat. Sol. (b), 58, 277–292.
THIESSEN, P. A. & MOLIÈRE, K. (1939). Ann. Phys. 34, 449–460.
VAN DER BIEST, O. & THOMAS, G. (1974). Phys. Stat. Sol. In the press.
WHELAN, M. J. & HIRSH, P. B. (1957). Phil. Mag. 2, 1121–1142.

Schwinger and Anomalous Scattering of Neutrons from CdS*

BY G. P. FELCHER AND S. W. PETERSON

Argonne National Laboratory, Argonne, Illinois 60439, U.S.A.

Polarization-sensitive neutron scattering from CdS single crystals has been observed for several Bragg reflections. This effect arises from interference between neutron spin–neutron orbit (Schwinger) scattering and 90° phase-shifted scattering due to such sources as absorption and a noncentrosymmetric crystal structure. The observed flipping ratios are in excellent agreement with those calculated on the basis of the accepted conventions for the determination of absolute configuration by X-ray or neutron diffraction. Possible application of the Schwinger scattering to the routine determination of absolute configurations is discussed.

Introduction

Polarized neutron diffraction from vanadium crystals (Shull, 1963) has given evidence for a polarization-sensitive scattering amplitude that is both asymmetric and dephased by 90° with respect to 'normal' scattering. This effect (Schwinger scattering) has been attributed to a neutron spin–neutron orbit interaction with the atomic Coulomb field.

We have performed a similar experiment with a crystal of CdS, a system for which the Schwinger scattering terms of cadmium and sulfur combine with the imaginary components of the scattering amplitude due to the cadmium resonance absorption and the noncentric sulfur positions. The polarizationse-nsitive scattering was indeed readily observed and its amplitude found in good agreement with that calculated.